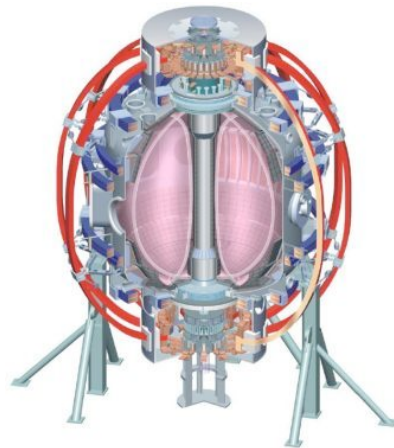


A few highlights from the EPS meeting in 2010

College W&M
Colorado Sch Mines
Columbia U
Comp-X
General Atomics
INL
Johns Hopkins U
LANL
LLNL
Lodestar
MIT
Nova Photonics
New York U
Old Dominion U
ORNL
PPPL
PSI
Princeton U
Purdue U
SNL
Think Tank, Inc.
UC Davis
UC Irvine
UCLA
UCSD
U Colorado
U Maryland
U Rochester
U Washington
U Wisconsin

Rajesh Maingi, 

37th EPS Meeting: Dublin, Ireland, 21-25 June 2010
NSTX physics meeting
June 28, 2010



Culham Sci Ctr
U St. Andrews
York U
Chubu U
Fukui U
Hiroshima U
Hyogo U
Kyoto U
Kyushu U
Kyushu Tokai U
NIFS
Niigata U
U Tokyo
JAEA
Hebrew U
Ioffe Inst
RRC Kurchatov Inst
TRINITI
KBSI
KAIST
POSTECH
ASIPP
ENEA, Frascati
CEA, Cadarache
IPP, Jülich
IPP, Garching
ASCR, Czech Rep
U Quebec

A few papers I will cover

- De Bock – **O2.107** – Edge Current Measurements using MSE during MAST H-modes
- Medvedev – **P4.145** – Free-boundary equilibrium and stability of snowflake diverted and negative triangularity plasmas in TCV
- Michael – **P1.1067** – Internal Transport Barrier in the MAST Spherical Tokamak
- Piras – **I5.115** Snowflake divertor experiments in NSTX

Electronic copies of first 2 in hand, and hardcopy of third one

- Conventional MSE can be used for edge current measurements in Spherical tokamaks (MAST ~ 2 ms)
- Neoclassical calculation yields lower and more narrow edge current layer than measurement. Just due to assumptions (e.g. $T_i = T_e$), or is neoclassical no longer valid in the edge ($\rho_\theta \sim L_n$)?
- Transient drop in $\max(j_{\phi, edge})$ when ∇p increases. Related to collisionality?

- Advantage of spherical tokamaks
 - Low B_ϕ at LFS, comparable to B_θ
 - Causes larger γ_m and larger changes in γ_m for similar changes in B_θ than in conventional tokamaks
 - e.g.

	Conventional tokamak	Spherical tokamak
B_θ	$0.2 T$	
ΔB_θ	$0.02 T$	
B_ϕ	$2.5 T$	$0.25 T$
$\gamma_m = \arctan(B_\theta/B_\phi)$	4.6°	38.7°
$\Delta \gamma_m = B_\phi / (B_\theta^2 + B_\phi^2) \Delta B_\theta$	0.46°	2.8°

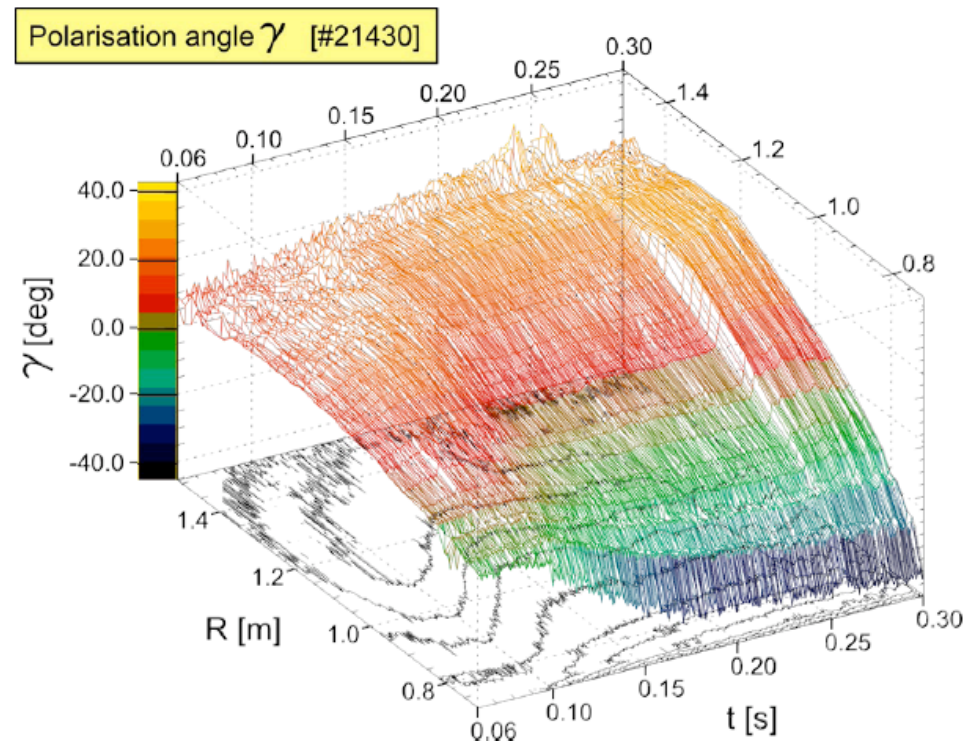
- MSE diagnostic at MAST²

- 35 channels,
- $\Delta R \sim 2.0\text{cm}$, $\Delta R/a \sim 2.8\%$
- Range = $0.7\text{m} - 1.5\text{m}$
– $-0.1 - 1.0$

- Core channels:
 $\sigma_{\gamma} \sim 0.5^{\circ}$ at $\Delta t = 0.5\text{ms}$

- Edge channels:
 $\sigma_{\gamma} \sim 0.5^{\circ}$ at $\Delta t = 2.0\text{ms}$

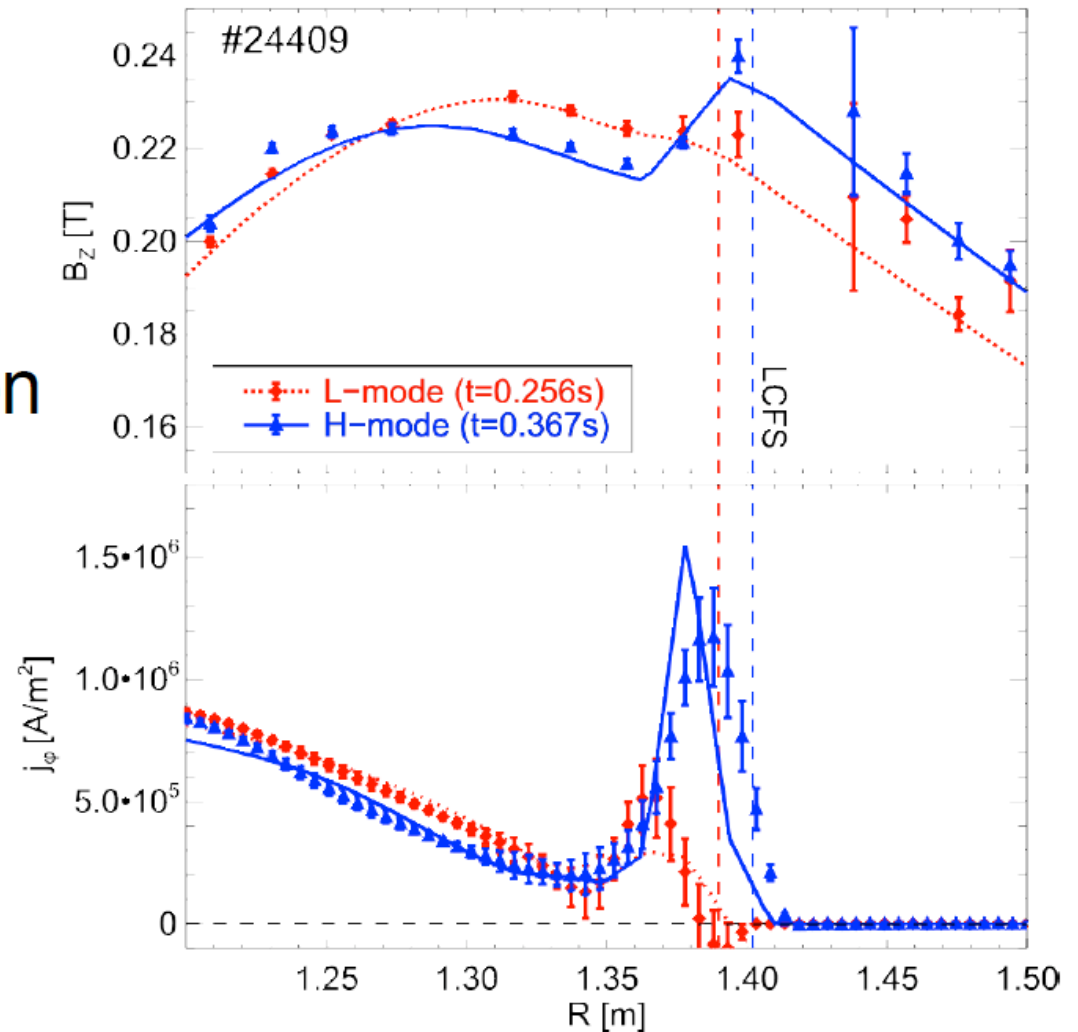
(e.g. due to lower signal levels at pedestal foot)



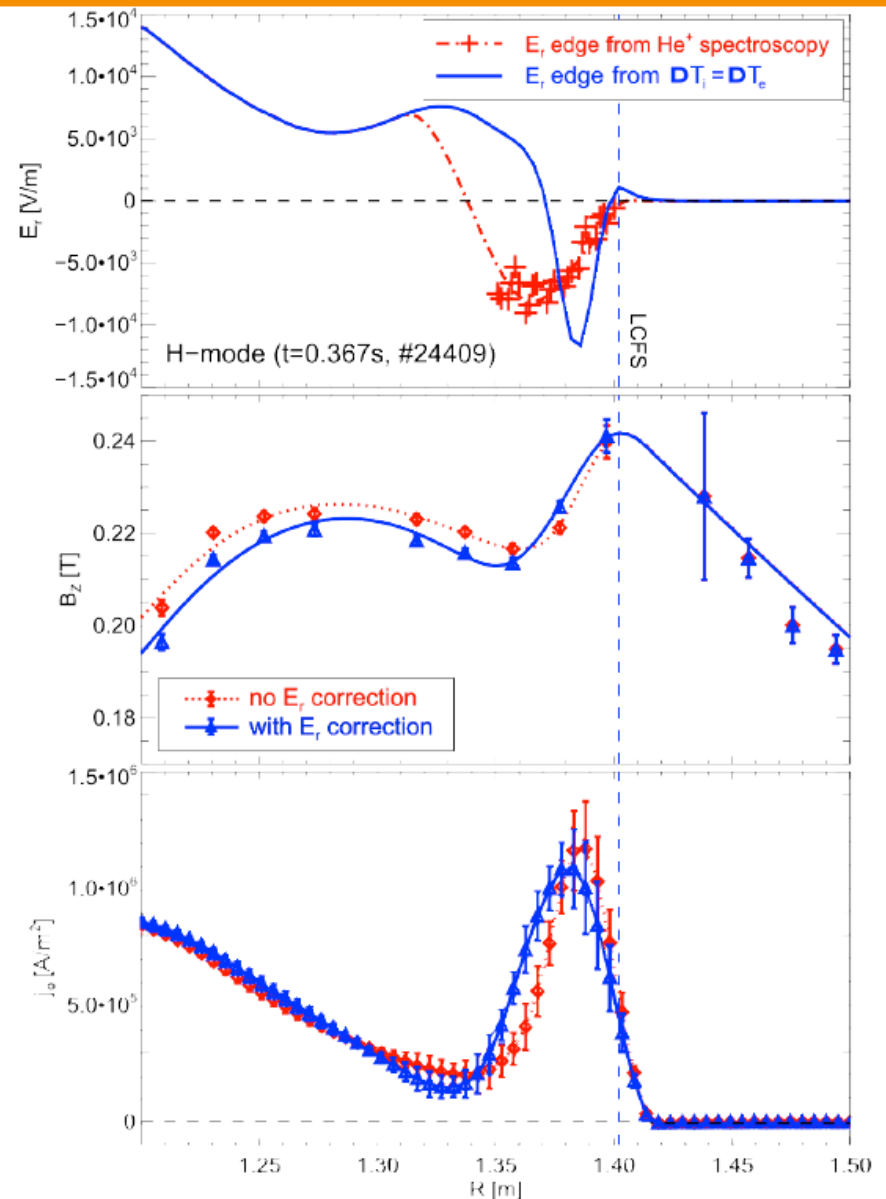
² M.F.M. De Bock, *et al.* Review of Scientific Instruments, 79(10):10F524, 2008
N.J. Conway, *et al.* Submitted to Review of Scientific Instruments, 2010

Strong edge current in H-mode

- L- and H-mode
- Comparison EFIT and direct calculation



- Effect of E_r is small in MAST
 - $\sim 2\%$ in B_z
 - $\sim 10\%$ in j_ϕ
- Correction...
 - Makes $\max(j_\phi)$ lower
 - Makes peak broader
 - Shifts peak inwards

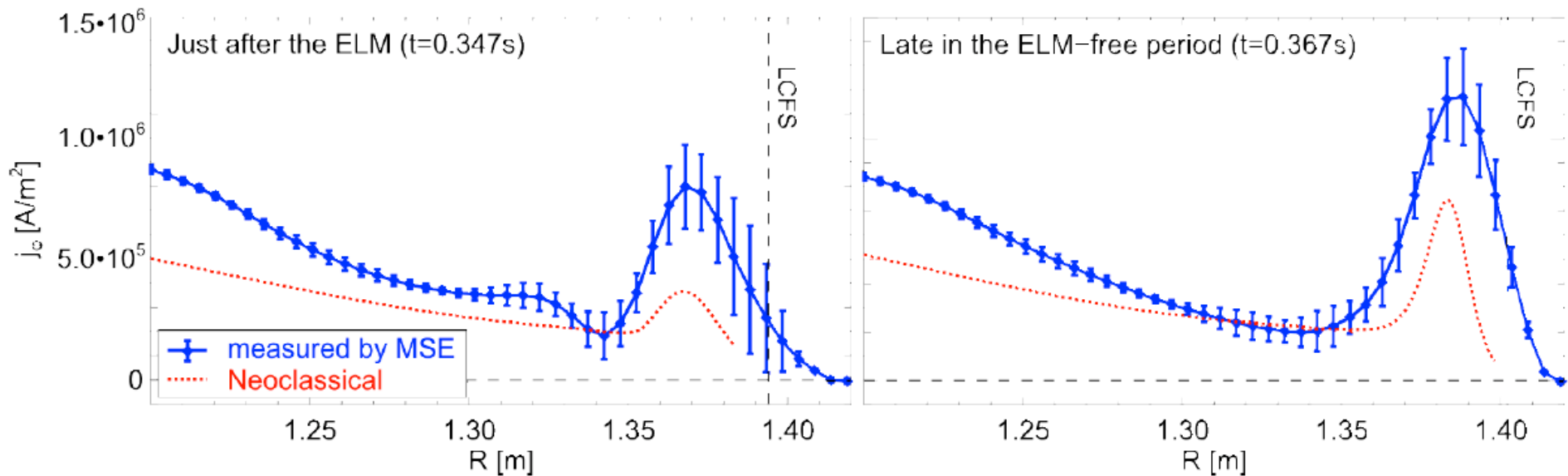


Comparison with neoclassical calculation

(11/17)

- Neoclassical calculation (bootstrap)

- Lower and narrower than measured

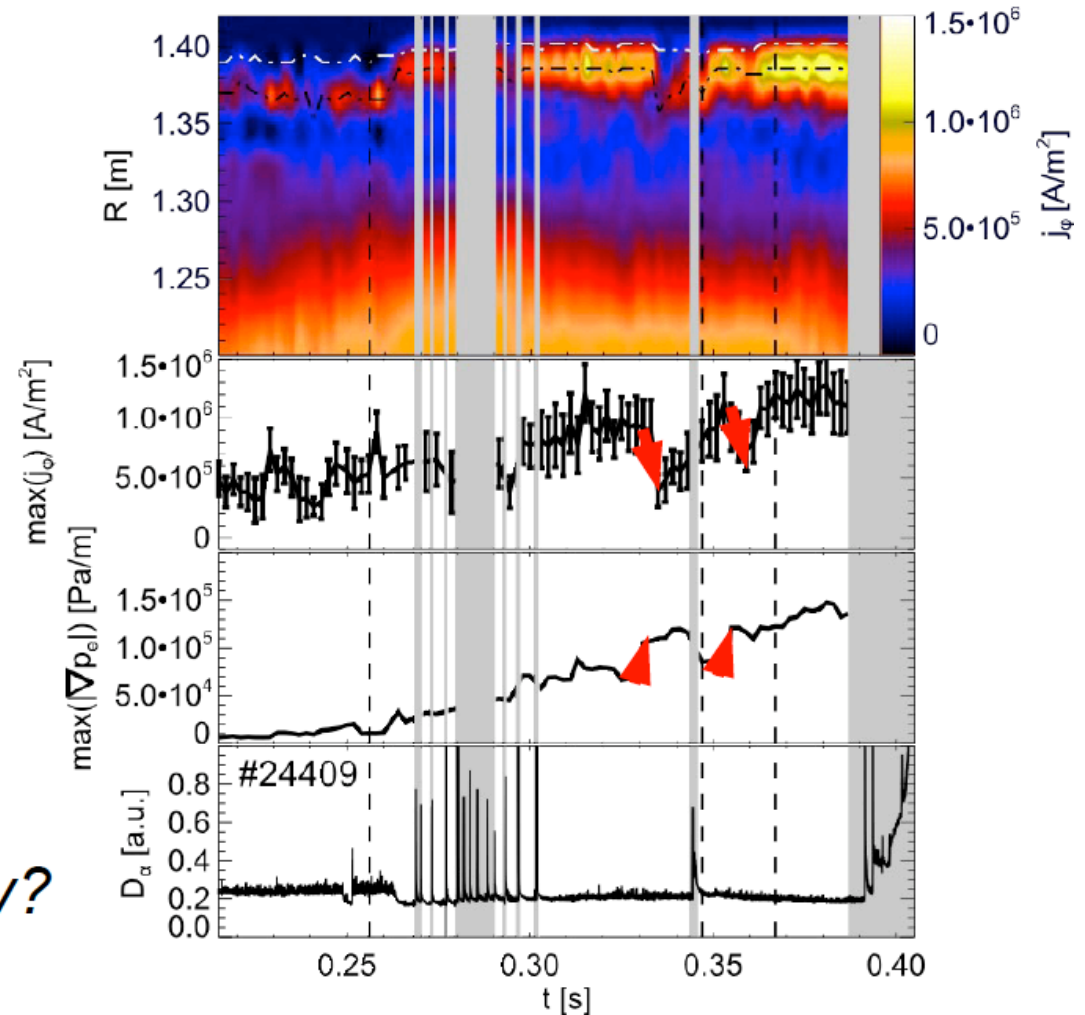


- $T_i = T_e$ and $n_i = n_e$ assumed, fitting of profiles, ...

- Spatial smoothing of MSE signal, ...

- Is neoclassical theory correct in the edge ($\rho_{\theta} \sim L_n$)? ...

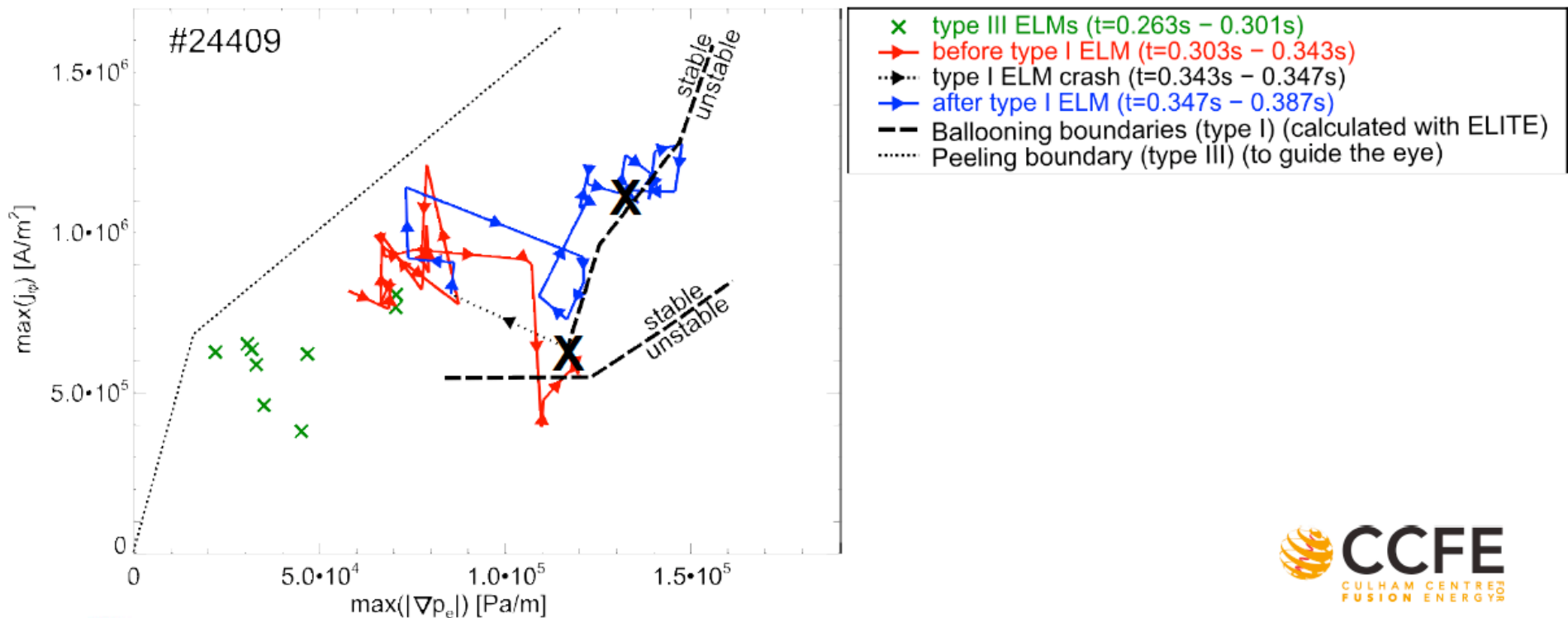
- Interesting:
 - Edge current 'ignores' the type I ELM *current diffusion timescales?*
 - Rise in pressure gradient seems to correlate with a transient drop in edge current *increased collisionality?*



Stability evolution and calculation

(15/17)

- Type III ELMs where peeling boundary is expected
- Type I ELMs occur when ballooning boundary ~crossed



Conclusions: SF with $\delta < 0$

- PF coil currents within TCV limits
 - Separatrix leg positions controlled
- High sensitivity of plasma shape to pedestal current density near null point
- Narrower plasma near null point with increasing pedestal current density
 - Better $n=0$ stability
 - Edge stability enhancement

SPIDER: Negative triangularity SN and SF equilibria ($I_p=380\text{kA}$)

Medvedev
P4.145

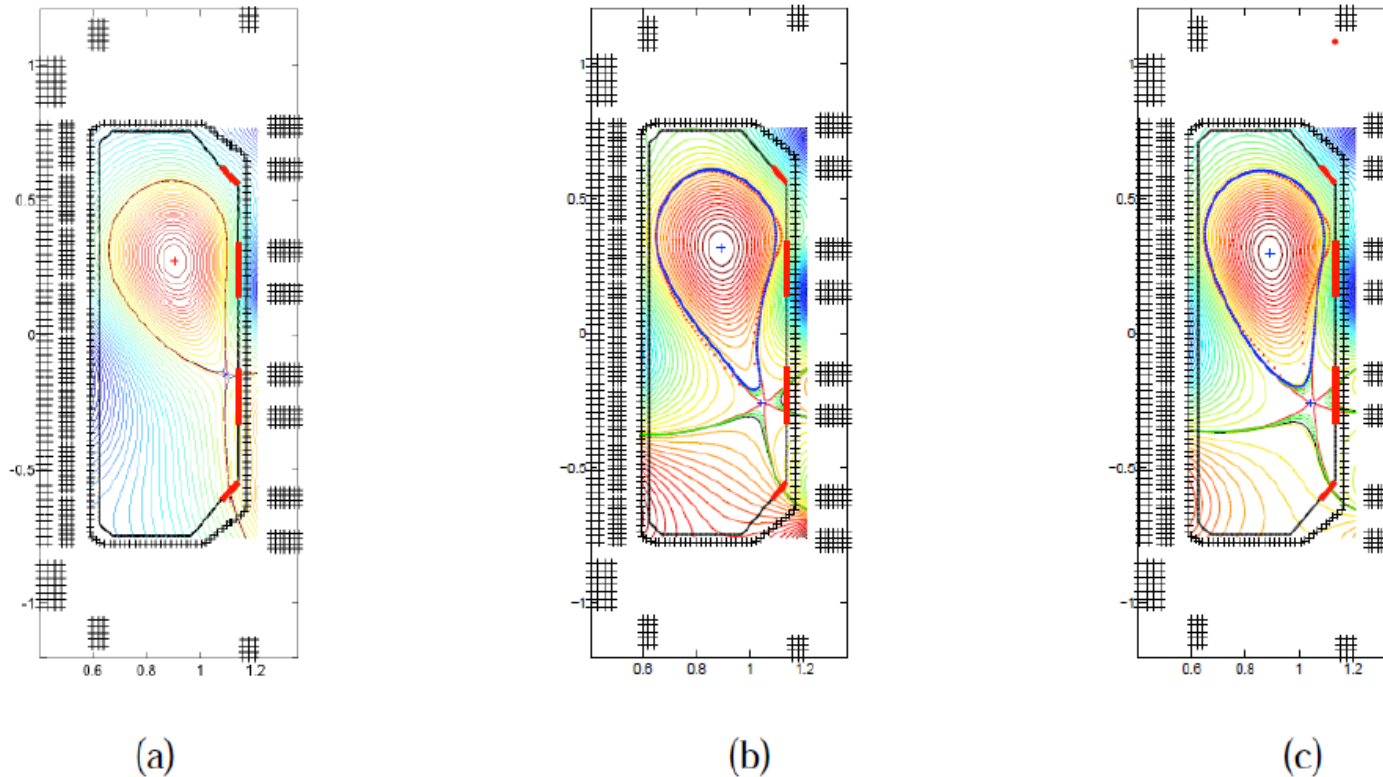
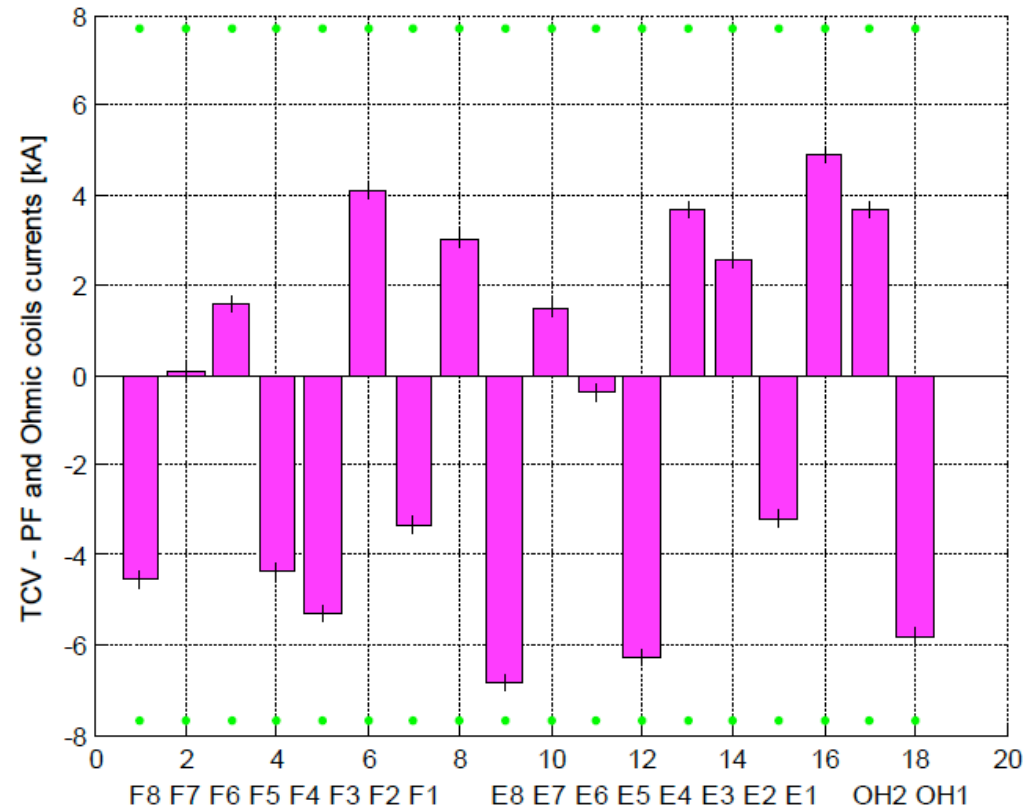
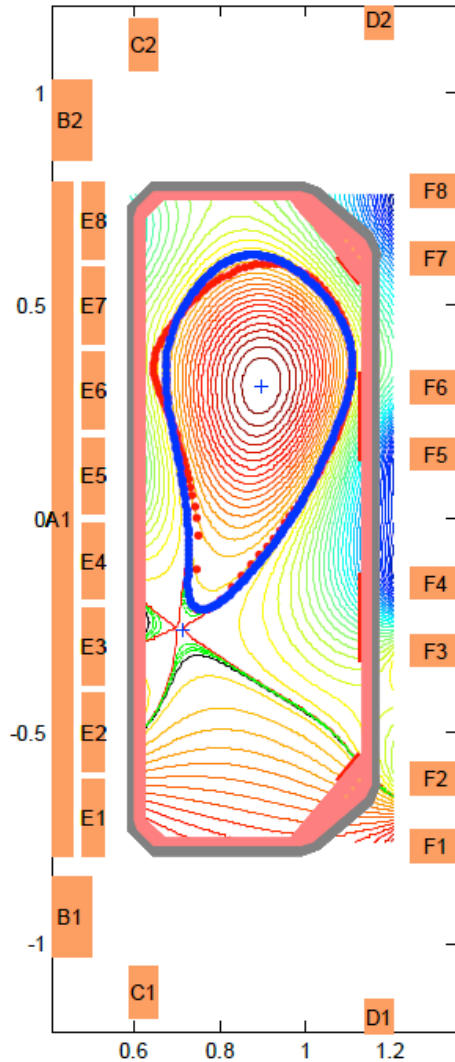
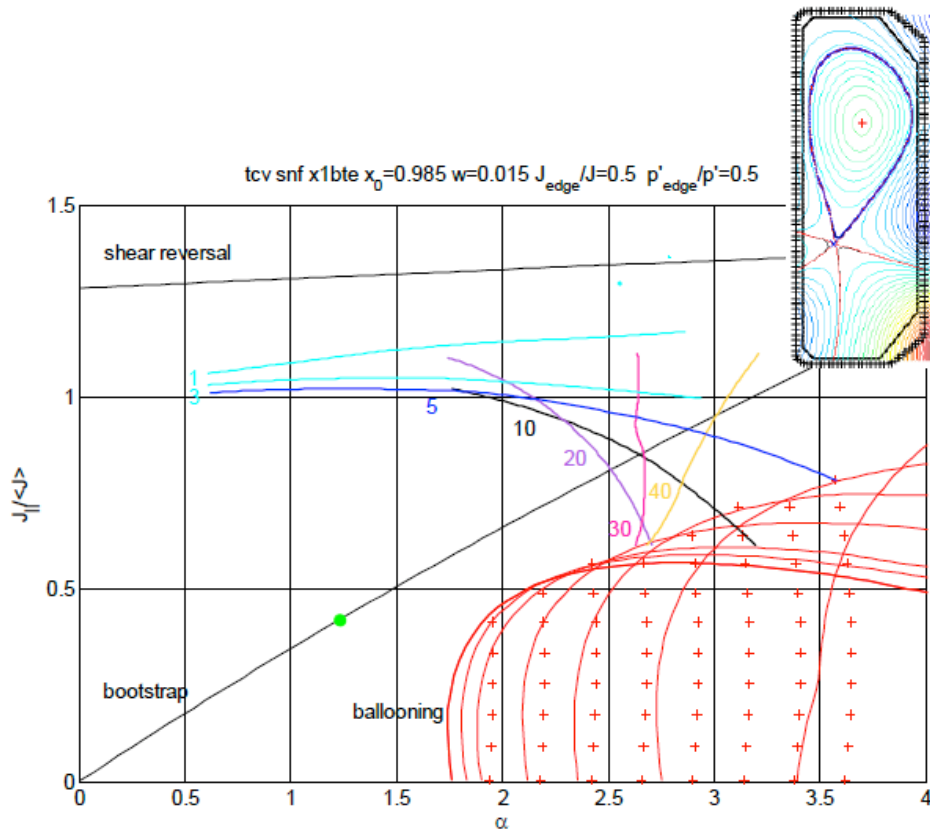


Figure 1. Free boundary equilibria with negative triangularity: single null (SN) with pedestal profiles (a), SF with pedestal profiles (b) and SF without pedestal (b). The positions of full toroidal coverage zones with graphite tiles are shown by thick red lines.

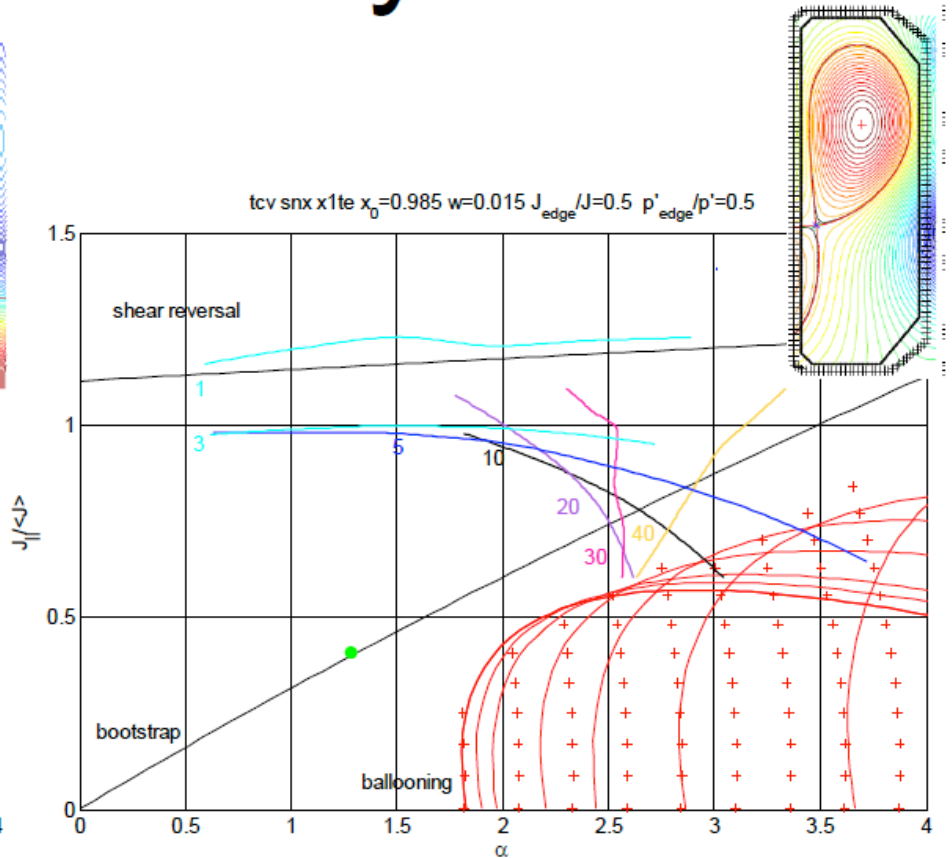
PF coil currents: SF positive δ



KINX edge stability: $\delta > 0$



Snowflake



X-point

F. Piras et al. Snowflake divertor experiments on TCV.
This conference **I5.115 Friday 10:40**

KINX edge stability: $\delta < 0$

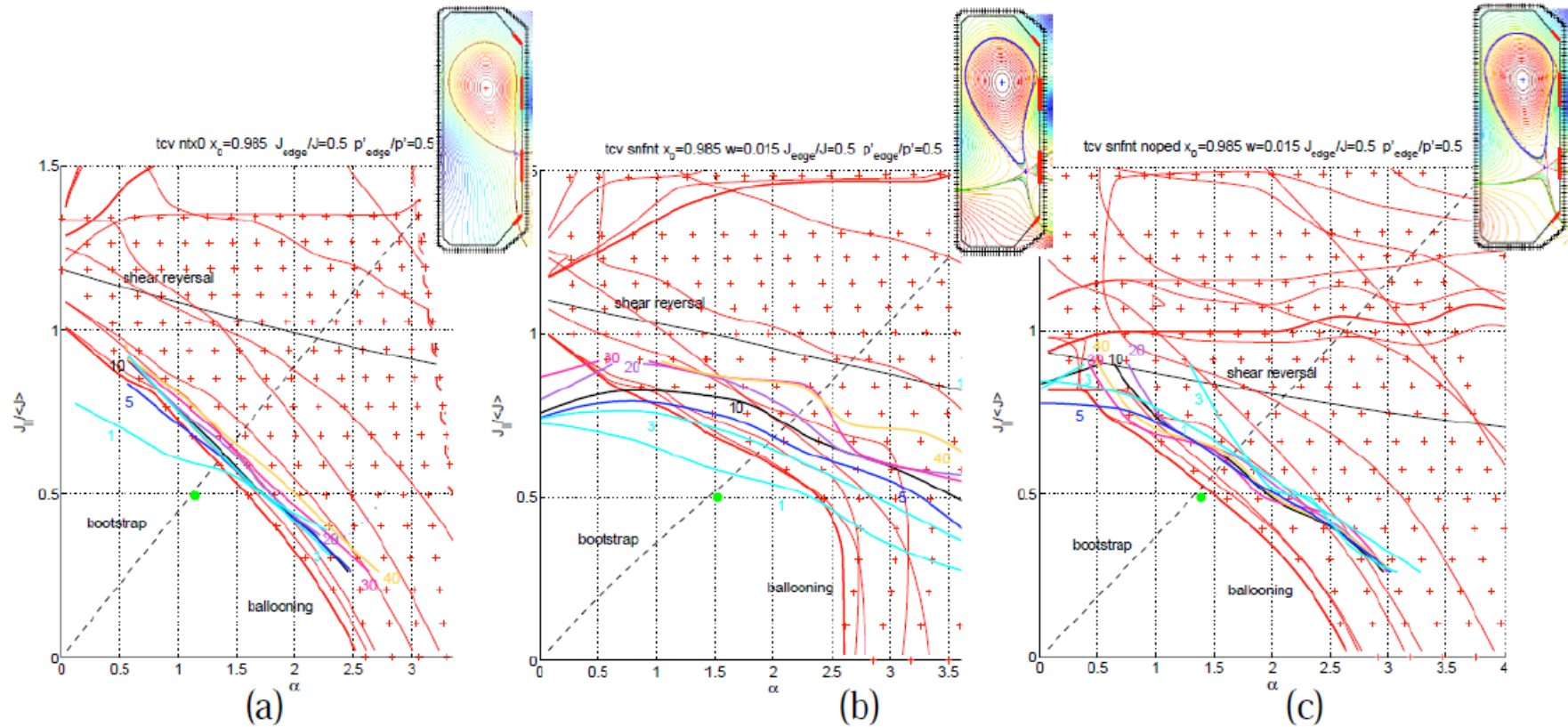
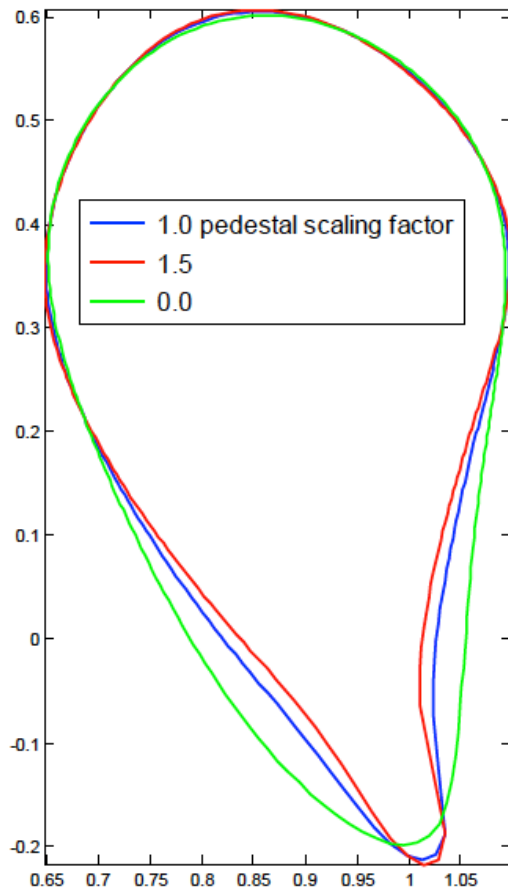


Figure 3. Edge stability diagrams for negative triangularity plasmas in TCV. The plasma shapes correspond to the free boundary equilibria from Fig.1.

Stability of self-consistent free boundary SF equilibria

Medvedev
P4.145



- Rescaling pressure gradient and current density in pedestal by the same factor
- Free-boundary equilibrium with prescribed null point position
- Stability limit enhancement compared to fixed boundary
 - $n=1$ mode: 1.2 to 1.25
 - $n=5$ mode: 1.4 to 1.6

Internal transport barriers dynamics in MAST

- Co- and counter ITBs build in early phases of discharge after favorable rotational shear profiles are established
- Mirnov signals:
 - Co: onset of fishbone/energetic instabilities at barrier time
 - Counter: quietening of fishbone/... at barrier time
- NBI modulation shows counter torque at mid radius by NBI
- Two barriers in counter: at q_{\min} and near $q=5/2$
 - Rotational shear weaker at the inner barrier
- Ultimately a LLM or tearing mode destroys the barrier
 - Tearing Mode locking condition is satisfied
- ETB formed some time after a mode destroys ITB and ITB moves its shear toward edge

Michael
P1.1067

Snowflake divertor experiments in TCV

- Established snowflake, snowflake +, and snowflake – (SFD) configurations
- Most comparisons between SFD, SFD+, and std. divertor
- Mostly magnetic topological changes quantified; no IR thermography data shown
- Confinement improved by 15%
- ELMs got less frequent and bigger on D_α